RSC Advances

Volume 1 | Number 1 | Jan 2013 | Pages 1–100

RSC Advances

www.rsc.org/advances

ROYAL SOCIETY OF CHEMISTRY

ROYAL SOCIETY OF CHEMISTRY

www.rsc.org/advances

Cite this: DOI: 10.1039/c0xx00000x

www.rsc.org/xxxxxx

**PAPER**

# Promoting effects of ceria on the catalytic performance of gold supported on $TiO_2$ for low-temperature CO oxidation

**Jun Yu,[ab] Guisheng Wu,[a] Guanzhong Lu,[*ab] Dongsen Mao[a] and Yun Guo[b]**

***Received (in XXX, XXX) Xth XXXXXXXXX 20XX, Accepted Xth XXXXXXXXX 20XX***

**DOI: 10.1039/b000000x**

The La or Ce-doped $TiO_2$ prepared by a sol-gel method was as the support, and supported gold catalysts for CO oxidation were prepared by the deposition-precipitation method. These Au catalysts were characterized by $N_2$ adsorption-desorption, ICP, XRD, TEM, $H_2$-TPR, and *in-situ* FT-IR. It was found that the doping of Ce or La in $TiO_2$ support can improve obviously the catalytic activity and stability of Au catalysts for CO oxidation, and the promoting effect of $CeO_2$ on its catalytic activity is much larger than $La_2O_3$. The presence of Ce can not only increase the surface area of $TiO_2$ and restrain the growth of $TiO_2$ crystallites, but also enhance the microstrain of $TiO_2$ and reinforce the interaction between $TiO_2$ and Au. As a result of the redox efficiency of $CeO_2$, the synergistic interaction between Au particles and support, the activity of active sites and the reactivity of surface oxygen species can be improved remarkably. Moreover, the effortless decomposition of carbonates and quick recovery of oxygen vacancies on the Au/Ce-$TiO_2$ surface might be responsible for the high stability of Au catalyst, comparing with the Au/$TiO_2$ catalyst.

## 1. Introduction

Gold as the catalyst component has attracted little attention during the development of heterogeneous catalysts over the past 50 years, because it is typically less catalytically active than other platinum group metals. However, when gold nano-particles are highly dispersed on different supports, it exhibits the surprisingly high activity for several reactions, such as methanol synthesis, water gas shift and automotive exhaust control,[1–6] in especial, the CO oxidation can occur at even below room temperature over nano-Au supported on $TiO_2$.[7–10] Therefore, a great number of investigations were employed to develop nano-gold catalysts, and to clarify the key influence factors on the catalytic activity of Au/$TiO_2$ for CO oxidation at low temperature. [11–16]

The research results show that the catalytic activity of Au/$TiO_2$ depends on the particle size of Au, physicochemical properties of the support and the interaction between Au particle and support. However the issue of active sites remains a matter of debate: some authors suggest that metallic gold is more active,[17–19] and others argue that oxidized gold is more active.[20–22] Up to now, the deactivation of nano-Au catalysts is still a great and insurmountable obstacle for the commercial application, for which some authors were attributed to sintering of gold particles, and other authors thought that the interaction between gold and $TiO_2$ plays a vital role in maintaining the high activity of Au/$TiO_2$.[14,16,23]

In order to further improve the catalytic activity and especially the stability of Au/$TiO_2$ catalysts, the surface modification of $TiO_2$ support was studied. Ma *et al.* studied the performance of Au/$TiO_2$ doped by rare earth (RE), and found that the addition of RE could retain excellent activity at ambient temperature, and enhance the dispersion of Au.[24] Since the high oxygen storage capacity and redox of ceria, the presence of ceria in Au/$CeO_2$/$SiO_2$ can affect the state and structure of the support and the interaction between gold and support.[25] Idakiev *et al.* reported that the ceria-modified $TiO_2$ is of much interest as potential support of gold-based catalyst for water-gas shift.[26] Recently, Li *et al.* studied that $CeO_2$ dominated in the Au/$CeO_2$-$TiO_2$ nanorods are able to promote the oxygen migration and gold dispersion, resulting in an evident increase of its catalytic activity for CO oxidation.[27] However, the promoting effect of RE additives proposed by the most of researchers was just attributed to its good thermal stability and high spontaneous dispersion,[24-28] the role of RE additives in the nature of active sites is still unclear and need to be investigated. Moreover, the comparison of stability of the gold catalysts supported on $TiO_2$ and RE-modified $TiO_2$ are also barely reported.

Herein, the composites of $La_2O_3$-$TiO_2$ and $CeO_2$-$TiO_2$ were prepared and then Au species were supported highly dispersedly on them, by which a high stable and long life Au/$TiO_2$ catalyst for CO oxidation was developed by an introduction of RE ions. And the role of RE in the Au/$La_2O_3$-$TiO_2$ and Au/$CeO_2$-$TiO_2$ catalysts was investigated, including the nature of active sites, the synergism between Au species and RE-modified support.

## 2. Experimental section

### 2.1. Catalyst preparation

$TiO_2$ was synthesized by the sol-gel method. 40 vol.% tetrabutyl titanate in anhydrous ethanol solution was dropped into the mixed solution (A) of 5 ml water, 10 ml acetic acid, and 25 ml anhydrous ethanol, under vigorous stirring at 40 °C, to obtain an opalescent solution. Subsequently, this solution was continually stirred at 60 °C to formation of gel. The formed gel was dried at 80 °C for 24 h and calcined in air at 550 °C for 6 h. After weighed lanthanum nitrate or cerium nitrate was dissolved in the solution (A), $La_2O_3$-$TiO_2$ or $CeO_2$-$TiO_2$ was synthesized by the same steps as $TiO_2$. The content of RE oxide was 5 wt.%.

NaOH aqueous solution of 1.0 mol/L was slowly dropped into 0.025 mol/L $HAuCl_4$ solution until pH = 7.0. Then $TiO_2$ (or $La_2O_3$-$TiO_2$, $CeO_2$-$TiO_2$) particles (> 200 mesh) were added to the above-mentioned solution under stirring, then this mixed solution was heated to 75 °C and aged for 2 h under continuous stirring, in which its pH value was kept to 7.0 by adding NaOH aqueous solution. The solid sample obtained was washed with deionized water several times until the $Cl^-$ ions cannot be observed in the wash solution, and then it was dried at 80 °C and calcined at 300 °C for 2 h. The obtained catalysts are denoted as Au/$TiO_2$, Au/$La_2O_3$-$TiO_2$ and Au/$CeO_2$-$TiO_2$, respectively.

### 2.2. Testing of the catalytic activity

A plug-flow fixed-bed reactor was used to test the activity of the catalysts for CO oxidation. 0.1g catalyst (60-80 mesh) was used. The reactant gases was consisted of 1 vol.% CO, 10 vol.% $O_2$, and 89 vol.% $N_2$, and its flow rate was 40 ml/min. The content of CO was analyzed by a gas chromatograph (GC) equipped with a thermal conductivity detector (TCD).

### 2.3. Catalyst characterization

The XRD patterns of samples were performed on a PANalytical X'Pert diffractometer with Ni β-filtered CuKα ($\lambda$ = 0.15418 nm) radiation at 40 kV and 40 mA. The mean crystallite size of the sample was estimated by Scherrer equation ($D = K\lambda/\beta\cdot\cos\theta$), and the microstrain of the sample was estimated by the equation of $\varepsilon = \beta/4\cdot\text{tg}\,\theta$, in which K is the constant related to the sample and experimental condition, λ is the diffraction wave length, β is the half high width, and θ is the diffraction angle. The surface areas of the catalysts were measured by $N_2$ adsorption at –196 °C on a Micrometrics ASAP 2020 M+C adsorption apparatus and calculated by Brumauer–Emmett–Teller (BET) method. Prior to $N_2$ adsorption, the catalysts were degassed under a vacuum of $10^{-1}$ Pa for 10 h at 200 °C. The content of Au in the catalyst was analyzed on an ICP-AES Philips PV8250 spectrometer. Transmission electron microscopy (TEM) images were obtained on a JEM-2100 electron microscope operated at 200 kV.

The $H_2$-temperature programmed reduction ($H_2$-TPR) of the samples was carried out in a quartz microreactor. 0.2 g catalyst (60-80 mesh) was used and pretreated in $N_2$ (40 ml/min) at 500 °C for 1 h. Subsequently, the temperature was dropped to room temperature, and the sample was heated in a flowing 10% $H_2$/$N_2$ stream (40 ml/min) up to 620 °C at 15 °C/min, in which a quadrupole mass spectrometer (QMS, OmniStar 200) was used as the detector to monitor the desorbed gases.

The *in-situ* FT-IR spectra of CO adsorbed on the catalyst were mearured on a Nicolet 6700 FT-IR spectrometer equipped with a diffuse reflectance infrared Fourier transform (DRIFT) cell with KBr windows. The sample in the cell was pretreated in $N_2$ (30 ml/min) at 300 °C for 2 h, and then the temperature was dropped to room temperature. After the cell was outgassed in vacuum to < $10^{-3}$ Pa, and the background was recorded. Following by introducing CO into the IR cell ($p_{co}$=8.0×$10^3$ Pa), the IR spectrum of CO adsorbed on the catalyst was recorded. The concentration of CO was higher than 99.97%, and it was pretreated by dehydration and deoxygenization before being used. The spectral resolution was 4 $cm^{-1}$ and the number of scans was 32.

## 3. Results and discussion

### 3.1. Catalytic activity for CO oxidation

The catalytic activities of Au/$TiO_2$, Au/$La_2O_3$-$TiO_2$ and Au/$CeO_2$-$TiO_2$ for CO oxidation are presented in Figure 1. Among three catalysts, Au/$TiO_2$ exhibits the lowest activity with $T_{50\%}$ (temperature of 50% CO conversion) of 38 °C and $T_{100\%}$ of 80 °C. Au/$CeO_2$-$TiO_2$ displays the highest catalytic activity, its $T_{100\%}$ is only –20 °C; next is Au/$La_2O_3$-$TiO_2$. These results show that $CeO_2$ and $La_2O_3$, especially $CeO_2$, are very effective promoters for the Au/$TiO_2$ catalyst.

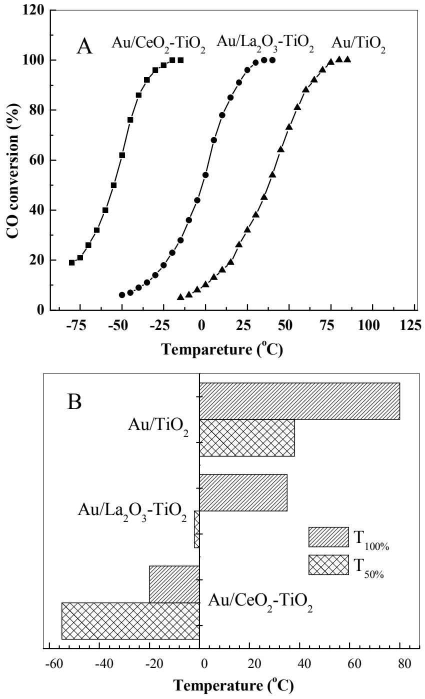

**Figure 1.** Catalytic preformances of Au/$TiO_2$, Au/$La_2O_3$-$TiO_2$ and Au/$CeO_2$-$TiO_2$ for CO oxidation

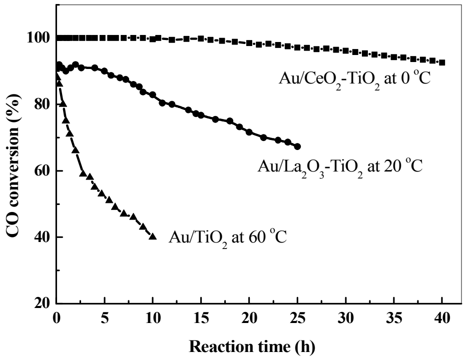

**Figure 2.** CO conversion as a function of time on stream over Au/$TiO_2$ at 60 °C, Au/$La_2O_3$-$TiO_2$ at 20 °C and Au/$CeO_2$-$TiO_2$ at 0 °C.

Figure 2 illustrates the relation between the catalytic activity and the reaction time over supported Au catalysts for CO oxidation. It can be seen that the catalytic activity of Au/$TiO_2$ displays a dramatic decrease at 60 °C with the reaction time, and decays by 48% after 8 h of reaction. It is interesting to note that the doping of rare earth additive can improve obviously the stability of Au/$TiO_2$. The Au/$CeO_2$-$TiO_2$ catalyst shows the highest stability among three catalysts, for instance, 100% CO conversion can be kept at 0 °C after 13 h of reaction, and only decays by 9% after 40 h of reaction.

### 3.2. Characterization of catalysts

The XRD patterns of catalysts are shown in Figure 3. The results show that there are the diffraction peaks of $TiO_2$ with the anatase-type structure, but no diffraction peaks of gold can be observed, indicating that the Au particles are highly dispersed on the supports due to lower content (0.28−0.42 wt.%, Table 1). With an addition of $La_2O_3$ or $CeO_2$, the diffraction peaks of $TiO_2$ are broadened obviously, that is, the grain size of $TiO_2$ becomes small and the microstrain of $TiO_2$ enhances (Table 1). It is conceivable that the formation of Ti-O-Ce (or La) bonds in the Ce(La)-$TiO_2$ can prevent the growth of $TiO_2$ grain. In addition, the diffraction peaks of $La_2O_3$ or $CeO_2$ cannot be also observed for Au/$La_2O_3$-$TiO_2$ and Au/$CeO_2$-$TiO_2$ catalysts, illustrating that $La_2O_3$ or $CeO_2$ in the catalysts is highly dispersed.

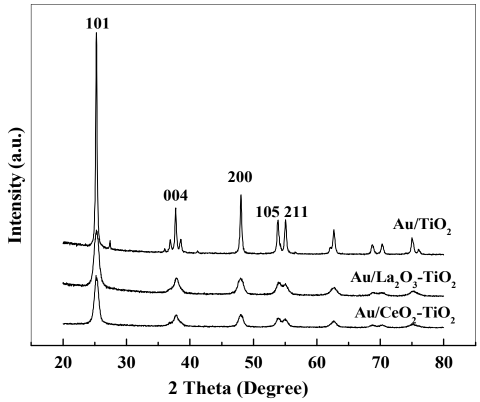

**Figure 3.** Powder XRD patterns of Au/$TiO_2$, Au/$La_2O_3$-$TiO_2$ and Au/$CeO_2$-$TiO_2$.

The TEM images of catalysts are shown in Figure 4. It can be seen that the grain sizes of Au/$TiO_2$ catalyst are very big and mainly 30–40 nm. For the Au/$La_2O_3$-$TiO_2$ and Au/$CeO_2$-$TiO_2$ catalysts, the doping of $La_2O_3$ or $CeO_2$ restrains the growth of $TiO_2$ crystallites, and its sizes are mainly 6–10 nm, which is in agreement with the result calculated by Scherrer equation on basis of the XRD patterns (Table 1). Meanwhile, the difference in grain size between different supports is also reflected by different specific surfaces areas (Table 1). Gold particles are homogeneously deposited on the supports. Compared with the Au/$TiO_2$ catalyst, it is obviously that the gold species on La- or Ce-modified $TiO_2$ tend to eventually form more ultrafine gold nanoparticles on its surface, due to the higher surface area and stronger interaction between adsorbed gold species and the support. In more detail, on smaller size particles of $La_2O_3$-$TiO_2$ or $CeO_2$-$TiO_2$ (Figure 4b, 4c), there are probably a large number of defects, such as oxygen vacancies, together with steps and adatoms on which gold immobilization could easily take place,[29] which is also in line with the data of Au loading (Table 1). Relating the activities of catalysts with their physicochemical properties, it is suggested that the promotion of the catalytic activity of Au/$La_2O_3$-$TiO_2$ and Au/$CeO_2$-$TiO_2$ should be attributed to an increase in the microstrain and Au loading (Table 1), compared with the Au/$TiO_2$ catalyst.

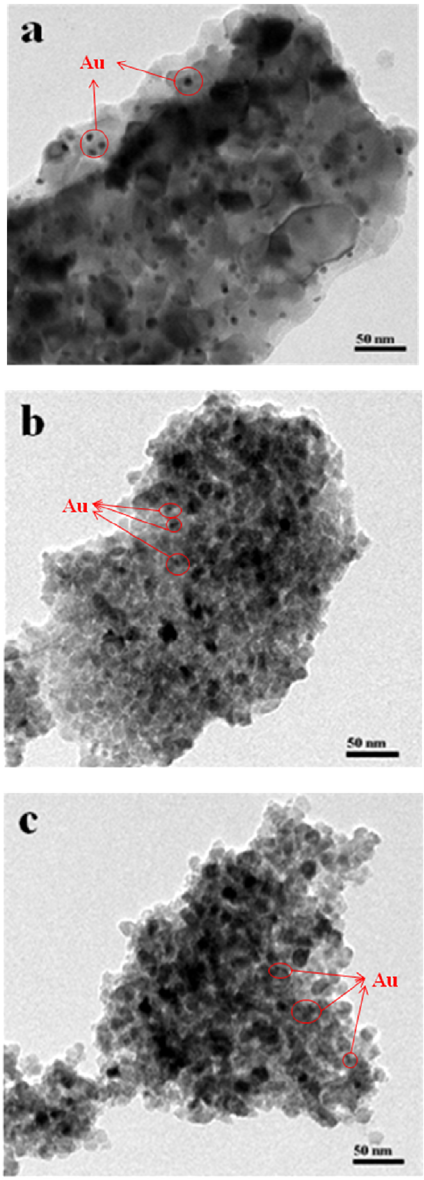

**Figure 4.** The TEM images of (a) Au/$TiO_2$, (b) Au/$La_2O_3$-$TiO_2$ and (c) Au/$CeO_2$-$TiO_2$ catalysts.

For the Au/$La_2O_3$-$TiO_2$ and Au/$CeO_2$-$TiO_2$ catalysts, there is no obvious difference between their physicochemical properties, such as the crystal size, microstrain, Au loading and BET surface area. However, the catalytic activity of Au/$CeO_2$-$TiO_2$ is much higher than that of Au/$La_2O_3$-$TiO_2$. These phenomenon shows that their differences in the catalyst structure alone are not enough to illustrate their differences in the catalytic activity for CO oxidation. To further investigate the interaction between gold particles and the corresponding supports, the $H_2$-TPR technique was employed, and the results are shown in Figure 5. It can be seen that pure $TiO_2$ is hardly reduced, and $La_2O_3$-$TiO_2$ and $CeO_2$-$TiO_2$ have a very weak reduction peak at 275~420 °C and 170~320 °C, respectively.

**Table 1.** Physicochemical properties of Au catalysts on different supports

| Catalyst | Au loading (wt.%) | $S_{BET}$ ($m^2/g$) | Crystal size (nm) | Microstrain (%) |
|---|---|---|---|---|
| Au/$TiO_2$ | 0.28 | 34 | 33.3 | 0.25 |
| Au/$La_2O_3$-$TiO_2$ | 0.40 | 71 | 8.5 | 0.94 |
| Au/$CeO_2$-$TiO_2$ | 0.42 | 65 | 8.9 | 0.93 |

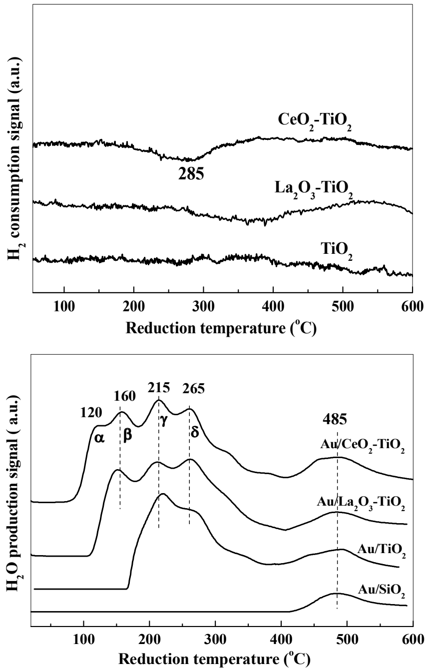

**Figure 5.** $H_2$-TPR-MS curves of the supports and Au catalysts on different supports.

After loading gold, there are a series of strong peaks at 100−300 °C, which are corresponding to the four overlapped reduction peaks (α, β, γ and δ), and a peak at 485 °C. Compared with the reduction peaks of Au supported on quartz, it is suggested that the peak at 485 °C is assigned to the reduction of Au oxide, and the peaks at 100~300 °C seem to be ascribed to the reduction of surface oxygen species of the supports promoted by Au species. Although the reduction peak of Au oxide species is similar for four samples, the reduction peaks at 100−300 °C are quite different from each other. Only Au/$TiO_2$ appears the γ and δ peaks, Au/$La_2O_3$-$TiO_2$ appears three peaks (β, γ and δ), and Au/$CeO_2$-$TiO_2$ shows four peaks (α, β, γ and δ). According to the results reported by Shapovalov *et al.*[30], the bond energy of oxygen on the surface of oxides can be weakened by the presence of Au species, indicating that the reduction peaks at 100~300 °C might be attributed to the reduction of surface oxygen species activated by gold species.

Furthermore, the presence of RE oxides can improve the properties of oxygen species on the $TiO_2$ surface, resulting in the variation of reducibility on the catalyst surface. As $CeO_2$ possesses a high oxygen storage capacity (OSC) and facile redox cycle of $Ce^{3+}/Ce^{4+}$,[25] the presence of $CeO_2$ can obviously increase the reactivity of oxygen species on the surface of catalyst and enhance the mobility of bulk oxygen in the catalyst. Thus, even compared with Au/$La_2O_3$-$TiO_2$, Au/$CeO_2$-$TiO_2$ may behave more active surface oxygen species by a variation of $Ce^{3+}/Ce^{4+}$, resulting in the presence of α peak in the TPR curve, that is to say, the surface oxygen species on Au/$CeO_2$-$TiO_2$ behaves the much lower reduction temperature than Au/$La_2O_3$-$TiO_2$.

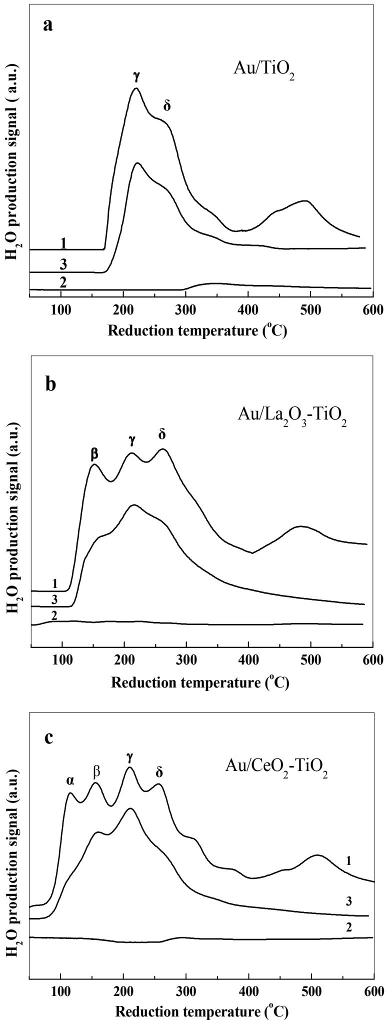

**Figure 6.** $H_2$-TPR-MS profiles of Au/$TiO_2$, Au/$La_2O_3$-$TiO_2$ and Au/$CeO_2$-$TiO_2$. (1) First TPR after the catalyst was treated in $N_2$ at 500 °C for 1 h; (2) following second TPR; (3) third TPR curve after the sample reduced by second TPR was exposed in $O_2$ at room temperature for 0.5 h.

To illustrate the redox property of the catalysts, the repeated TPR for the catalysts are investigated, and the results are presented in Figure 6. The results show that the second TPR of all samples does not display any reduction peaks because the surface oxygen species have been exhausted during the first TPR. After second TPR was finished, the samples were cooled in $N_2$ to room temperature and then exposed in the oxygen flow at room temperature for 30 min. The results of third TPR show that, the reduction peaks at 100−300 °C recur, but the peak intensities are relatively weaker and the reduction peak at 485 °C disappears. These results above indicate that the surface oxygen species on the supports can react with hydrogen by the help of Au, and the oxygen vacancies left can be restored in the oxygen flow at room temperature. Compared with the third TPR curves of Au/$TiO_2$

and $Au/La_2O_3$-$TiO_2$, $Au/CeO_2$-$TiO_2$ still holds the strongest oxygen adsorption ability and possesses the most active oxygen species (as the α peak), although the α peak in third TPR curve is smaller than that in first TPR curve.

### 3.3. CO adsorption on different samples

The CO adsorption on $Au/TiO_2$, $Au/La_2O_3$-$TiO_2$ and $Au/CeO_2$-$TiO_2$ were investigated by *in-situ* FT-IR technique, and the results are shown in Figure 7. The band at 2112 $cm^{-1}$ on $Au/TiO_2$ should be ascribed to linear CO species adsorbed on the $Au^0$ sites,[31,32] and this band on $Au/La_2O_3$-$TiO_2$ and $Au/CeO_2$-$TiO_2$ is shifted to 2118 $cm^{-1}$. Meanwhile, the new peaks at 2133 and 2154 $cm^{-1}$ appear on the $Au/La_2O_3$-$TiO_2$ and $Au/CeO_2$-$TiO_2$ catalysts. In general, the blue shift of carboxylic stretching usually indicates that the Au electrodes shift to a positive potentials, and the bands at 2155-2130 $cm^{-1}$ is ascribed to the feature band of carbonyls on positively charged gold species[33-35] or gold atoms with adsorbed oxygen[36–38]. Compared with the $Au/La_2O_3$-$TiO_2$ catalyst, the peak at 2154 $cm^{-1}$ only appears on $Au/CeO_2$-$TiO_2$, and $Au/CeO_2$-$TiO_2$ has still a stronger absorption band at 2133 $cm^{-1}$. It is conceivable that $Au/CeO_2$-$TiO_2$ holds the more active surface oxygen species interacted with the Au particles, which is consistent with the result of $H_2$-TPR. Besides, the weak peak at 2186 $cm^{-1}$ on $Au/CeO_2$-$TiO_2$ is assigned to linear CO species adsorbed on $Ti^{\delta+}$ cations.[39, 40]

For $Au/La_2O_3$-$TiO_2$ and $Au/CeO_2$-$TiO_2$, there are a series of strong bands at 1670, 1586, 1425, 1246 $cm^{-1}$, which are assigned to the bidentate and monodentate carbonate species adsorbed on the surface,[41,42] and these absorption peaks cannot be observed on $Au/TiO_2$.

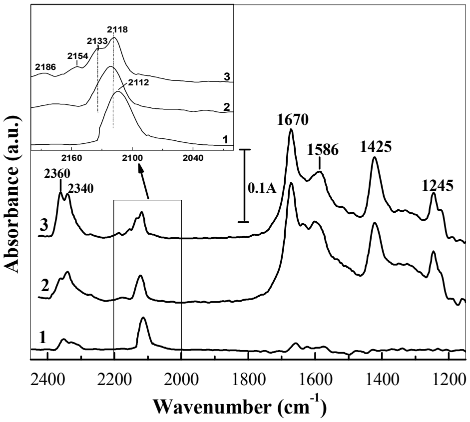

**Figure 7** *in-situ* FT-IR absorption spectra of CO (80 mbar) adsorbed on (1) $Au/TiO_2$, (2) $Au/La_2O_3$-$TiO_2$, and (3) $Au/CeO_2$-$TiO_2$.

## 4. Discussion

### 4.1. Structure-activity relation

The results of XRD, TEM and BET surface area show that, the presence of $La_2O_3$ or $CeO_2$ can restrain the growth of $TiO_2$ crystallites, and increase the surface area and microstrain of $TiO_2$ support, which promotes an interaction between the Au species and support and causes the presence of Au species at smaller size. As CO oxidation may happen in the interface between Au particles and $TiO_2$,[14] an introduction of $CeO_2$ and $La_2O_3$ can improve the catalytic activities of active sites, resulting in the high activity of $Au/La_2O_3$-$TiO_2$ and $Au/CeO_2$-$TiO_2$.

### 4.2. The nature of active sites

The comparison of the activities of $Au/La_2O_3$-$TiO_2$ and $Au/CeO_2$-$TiO_2$ with the results of $H_2$-TPR and CO adsorption can reveal that, in addition to the crystal size and surface area of the support, other factors, such as the redox property of sample and the oxidation state of dispersed Au particles may also influence their catalytic activities. The TPR results (Figures 5 and 6) show that, there are a variety of surface oxygen species on the surface of $TiO_2$ support, which are facile to be reduced by the help of Au species at 100-300 °C. Furthermore, after the reduced catalysts re-adsorbs $O_2$ at room temperature, the reduction peaks at low temperature can be recovered, indicating that the oxygen vacancies formed by the reduction of hydrogen can be restored in the atmosphere containing oxygen. The presence of $CeO_2$ in $TiO_2$ support makes the $Au/CeO_2$-$TiO_2$ catalyst possess very strong oxygen adsorption ability and active surface oxygen species, which is a crucial factor with regard to the high efficient catalyst for low-temperature CO oxidation.[12,15]

*in-situ* FT-IR absorption spectra of CO adsorption (Figure 7) reveal also that the carboxylic stretching absorption peaks on $Au/La_2O_3$-$TiO_2$ and $Au/CeO_2$-$TiO_2$ are blue shifted compared with that on $Au/TiO_2$, and the absorption bands of carbonyls on the $(Au_n)^{\delta+}$ sites at 2160-2125 $cm^{-1}$ appear for the $Au/La_2O_3$-$TiO_2$ and $Au/CeO_2$-$TiO_2$ catalysts, which indicates that the more positively charged Au species are existed on these catalysts due to the presence of $CeO_2$ or $La_2O_3$. This is because that the doping of Ce or La is conducive to a formation of the $(Au_n)^{\delta+}$ sites with the help of surface oxygen species.[43] Among the rare earth elements, $CeO_2$ has a unique redox property and high oxygen storage capacity (OSC), and is the best promoter of oxygen properties (as mobility and reactivity) for the transition metal oxide catalysts. Therefore, much more active sites of $(Au_n)^{\delta+}$ can be formed on the surface of $Au/CeO_2$-$TiO_2$, and play a very important role in improving catalytic activity for low-temperature CO oxidation.

### 4.3. Reaction mechanism and role of Ce

CO oxidation on a supported gold catalyst occurs on the Au perimeter or Au–support interface.[44] The oxygen atoms from the oxide support play a role in the binding of Au particles, and supply oxygen species for the CO oxidation. On the basis of previous investigation,[45] a model of CO oxidation mechanism can be proposed as Figure 8.

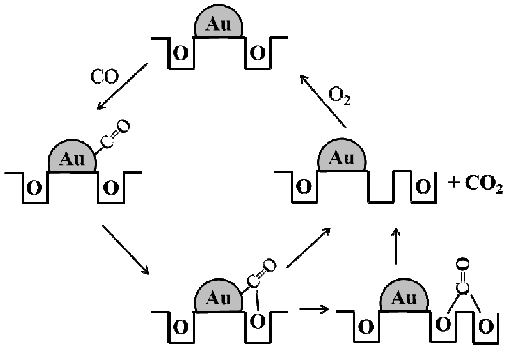

**Figure 8.** Mechanism of CO oxidation over supported Au catalyst

The first step is CO adsorption on the gold particle, and then the surface carbonyl on the gold particle migrates to the Au–support boundary to transform into an active intermediate. The intermediate may be converted into carbonate-like surface species unceasingly. Once this active intermediate decomposes to $CO_2$ product, the active site can be liberated, and adsorption of gaseous oxygen can take place, resulting in restoration of the surface oxygen vacancies.

As the carbonate species formed on the surface of catalyst would prevent formation of the active intermediate (or complex), it is in general illustrated as the deactivation of $Au/TiO_2$.[10,11] Based on the results of $H_2$-TPR and *in situ* FT-IR, it is proposed that the Ce-modified $Au/TiO_2$ possesses very strong oxygen adsorption ability and the active oxygen species at low temperatures. As a result, carbonates can be easily decomposed to release $CO_2$ on the Ce-doped surface and the oxygen vacancies can be also readily formed or restored. The more stability of $Au/CeO_2$-$TiO_2$ catalyst should be attributed to the oxygen-enriched interface and strong synergy of Au-support due to the doping of Ce. Therefore, the presence of Ce (La) improves the catalytic performance and stability of the $Au/TiO_2$ catalyst.

## 5. Conclusions

In summary, a high stable and long life $Au/CeO_2$-$TiO_2$ catalyst for CO oxidation was successfully developed and prepared, and the doping of cerium or lanthanum can obviously improve the catalytic activity for CO oxidation and the effect of $CeO_2$ on its catalytic activity is much larger than $La_2O_3$. The research results show that doping of RE oxide can increase the specific surface area, restrain the growth of the grains, and enhance the microstrain of $TiO_2$, resulting in reinforcing the interaction between gold species and the support, and higher dispersion of Au particles on the support.

The doping of ceria or lanthanum oxide can improve the synergistic interaction between support and Au particles, and enhance the reactivity of the surface oxygen species of the catalyst. Because of the redox properties of ceria and more rich surface oxygen species on $CeO_2$-$TiO_2$, more active sites of $(Au_n)^{\delta+}$ can be formed, resulting in a higher catalytic activity over $Au/CeO_2$-$TiO_2$. Moreover, it is clearly revealed that the effortless decomposition of carbonates and quick recovery of oxygen vacancies caused by the modification of Ce might be responsible for the high stability of $Au/CeO_2$-$TiO_2$.

## Acknowledgements

This project was financially supported by the National Natural Science Foundation of China (21273150), the National Basic Research Program of China (2010CB732300, 2013CB933201), the national high technology research and development program of China (2011AA03A406, 2012AA062703), the Fundamental Research Funds for the Central Universities, the "ShuGuang" Project (10GG23) of Shanghai Municipal Education Commission and Shanghai Education Development Foundation.

## Notes and references

*a Research Institute of Applied Catalysis, School of Chemical and Environmental Engineering, Shanghai Institute of Technology, Shanghai 201418, P. R. China. Fax: +86-21-60879111 E-mail: gzhlu@ecust.edu.cn (G.Z. LU).*

*[b] Key Laboratory for Advanced Materials and Research Institute of Industrial catalysis, East China University of Science and Technology, Shanghai 200237, P. R. China. Fax: +86-21-64253824*

1 G.C. Bond, D.T. Thompson, *Catal. Rev. Sci. Eng.*, 1999, **41**, 319.
2 W.G. Menezes, V. Zielasek, K. Thiel, A. Hartwig, M.B. Bäumer, *J. Catal.*, 2013, **299**, 222.
3 M.C. Daniel, D. Astruc, *Chem. Rev.*, 2004, **104**, 293.
4 C.W. Corti, R.J. Holliday, D.T. Thompson, *Appl. Catal. A: Gen.*, 2005, **291**, 253.
5 D.H. Son, S.M. Hughes, Y.D. Yin, A.P. Alivisatos, *Science*, 2004, **306**, 1009.
6 M. Ojeda, B.Z. Zhan, E. Iglesia, *J. Catal.*, 2012, **285**, 92.
7 G.C. Bond, D.T. Thompsom, *Gold Bull.*, 2000, **33**, 41.
8 W.K. Li, L.N. Chu, X.Q. Gong, G.Z. Lu, *Surf. Sci.*, 2011, **605**, 1369.
9 M.S. Chen, D.W. Goodman, *Science*, 2004, **306**, 252.
10 J. Saavedra, C. Powell, B. Panthi, C.J. Pursell, B.D. Chandler, *J. Catal.*, 2013, **307**, 37.
11 T.A. Ntho, J.A. Anderson, M.S. Scurrell, *J.Catal.*, 2009, **261**, 94.
12 L.M. Liu, B. Mcallister, H.Q. Ye, P. Hu, *J. Am. Chem. Soc.*, 2006, **128**, 4017.
13 A. Chiorino, M. Manzoli, F. Menegazzo, M. Signoretto, F. Vindigni, F. Pinna, F. Boccuzzi, *J. Catal.*, 2009, **262**, 169.
14 M. Comotti, W.C. Li, B. Spliethoff, F. Schüth, *J. Am. Chem. Soc.*, 2006, **128**, 917.
15 M. Kotobuki, R. Leppelt, D.A. Hansgen, D. Widmann, R.J. Behm, *J. Catal.*, 2009, **264**, 67.
16 H.H. Kung, M.C. Kung, C.K. Costello, *J. Catal.*, 2003, **216**, 425.
17 M. Daté, H. Imai, S. Tsubota, M. Haruta, *Catal. Today*, 2007, **122**, 222
18 M.A.P. Dekkers, M.J. Lippits, B.E. Nieuwenhuys, *Catal. Lett.*, 1998, **56**, 195.
19 F. Boccuzzi, A. Chiorino, M. Manzoli, P. Lu, T. Akita, S. Ichikawa, M. Haruta, *J. Catal.*, 2001, **202**, 256.
20 S. Minicò, S. Scirè, C. Crisafulli, S. Gavagno, *Appl. Catal. B: Environ.*, 2001, **34**, 277.
21 J.L. Margitfalvi, A. Fási, M. Hegedűs, F. Lónyi, S. Gőbölös, N. Bogdanchikova, *Catal. Today*, 2002, **72**, 157.
22 M.S. Chen, D.W. Goodman, *Catal. Today*, 2006, **111**, 22.
23 M. Haruta, *Gold Bull.*, 2004, **37**, 27.
24 Z. Ma, S.H. Overbury, S. Dai, *J. Mol. Catal. A: Chem.*, 2007, **273**, 186.
25 K. Qian, S.S. Lv, X.Y. Xiao, H.X. Sun, J.Q. Lu, M.F. Luo, W.X. Huang, *J. Mol. Catal. A: Chem.*, 2009, **306**, 40.
26 V. Idakiev, T. Tabakova, K. Tenchev, Z.Y. Yuan, T.Z. Ren, B.L. Su, *Catal. Today*, 2007, **128**, 223.
27 S. Li, H.Q. Zhu, Z.F. Qin, G.F. Wang, Y.G. Zhang, Z.W. Wu, Z.K. Li, G. Chen, W.W. Dong, Z.H. Wu, L.R. Zheng, J. Zhang, T.D. Hu, J.G. Wang, *Appl. Catal. B: Environ.*, 2014, **144**, 498.
28 N. Sahu, K.M. Parida, A.K. Tripathi, V.S. Kamble, *Appl. Catal. A: Gen.*, 2011, **399**, 110.
29 N. Lopez, J.K. Nørskov, T.V.W. Janssens, A. Carlsson, A. Puig-Molina, B.S. Calusen, J.-D. Grunwaldt, *J. Catal.*, 2004, **225**, 86.
30 V. Shapovalov, H. Metiu, *J. Catal.*, 2007, **245**, 205.
31 S. Minico, S. Scire, C. Crisafalli, A.M. Visco, S. Galvagno, *Catal. Lett.*, 1997, **47**, 273.
32 F. Boccuzzi, A. Chiorino, M. Manzoli, *Surf. Sci.*, 2000, **454-456**, 942.
33 T. Tabakova, F. Boccuzzi, M. Manzoli, J.W. Sobczak, V. Idakiev, D.Andreeva, *Appl. Catal. B: Environ.*, 2004, **49**, 73.
34 Tz. Venkov, K. Fajerwerg, L. Delannoy, Hr. Klimev, K. Hadjiivanov, C. Louis. *Appl. Catal. A: Gen.*, 2006, **301**, 106.
35 Tz. Venkov, Hr. Klimev, M.A. Centeno, J.A. Odriozola, K. Hadjiivanov. *Catal. Commun.*, 2006, **7**, 308.
36 F. Boccuzzi, A. Chiorino, *J. Phys. Chem. B*, 2000, **104**, 5414.
37 J.-D. Grunwaldt, M. Maciejewski, O. Becker, P. Fabrizioli, A. Baiker, *J. Catal.*, 1999, **186**, 458.
38 D. Guillemot, V. Borokov, V. Kazansky, M. Polisset-Thfoin, J. Fraissard. *J. Chem. Soc. Faraday Trans.*, 1997, **93**, 3587.

39 M.A. Centeno, K. Hadjiivanov, Tz. Venkov, Hr. Klimev, J.A. Odriozola, *J. Mol. Catal. A: Chem.*, 2006, **252**, 142.
40 F. Boccuzzi, A. Chiorino, S. Tsubota, M. Haruta, *J. Phys. Chem.*, 1996, **100**, 3625.
41 M.J. Pollard, B.A. Weinstock, T.E. Bitterwolf, P.R. Griffiths, A.P. Newbery, J.P. Paine, *J. Catal.*, 2008, **254**, 218.
42 M.A. Debeila, R.P.K. Wells, J.A. Anderson. *J. Catal.*, 2006, **239**, 162.
43 J. Yu, G.S. Wu, D.S. Mao, G.Z. Lu, *Acta. Phys.-Chim. Sin.*, 2008, **24**, 1751.
44 Y.Y. Wu, N.A. Mashayekhi, H.H. Kung, *Catal. Sci. Technol.*, 2013, **3**, 2881.
45 P. Konova, A. Naydenov, Cv. Venkov, D. Mehandjiev, D. Andreeva, T. Tabakova, *J. Mol. Catal. A: Chem.*, 2004, **213**, 235.

## Graphical abstract

# Promoting effects of ceria on the catalytic performance of gold supported on $TiO_2$ for low-temperature CO oxidation

Jun Yu, Guisheng Wu, Guanzhong Lu, * Dongsen Mao and Yun Guo

The doping of Ce enhanced the Au-support synergy and modified the active sites. The effortless decomposition of carbonates and quick recovery of oxygen vacancies on the $Au/CeO_2$-$TiO_2$ surface should be responsible for its high stability.